

**Zeitschrift:** IABSE congress report = Rapport du congrès AIPC = IVBH  
Kongressbericht

**Band:** 12 (1984)

**Artikel:** Computer-aided design of box girders using a simple non-linear  
technique

**Autor:** Cusens, A.R. / Lengyel, P.

**DOI:** <https://doi.org/10.5169/seals-12152>

### **Nutzungsbedingungen**

Die ETH-Bibliothek ist die Anbieterin der digitalisierten Zeitschriften auf E-Periodica. Sie besitzt keine Urheberrechte an den Zeitschriften und ist nicht verantwortlich für deren Inhalte. Die Rechte liegen in der Regel bei den Herausgebern beziehungsweise den externen Rechteinhabern. Das Veröffentlichen von Bildern in Print- und Online-Publikationen sowie auf Social Media-Kanälen oder Webseiten ist nur mit vorheriger Genehmigung der Rechteinhaber erlaubt. [Mehr erfahren](#)

### **Conditions d'utilisation**

L'ETH Library est le fournisseur des revues numérisées. Elle ne détient aucun droit d'auteur sur les revues et n'est pas responsable de leur contenu. En règle générale, les droits sont détenus par les éditeurs ou les détenteurs de droits externes. La reproduction d'images dans des publications imprimées ou en ligne ainsi que sur des canaux de médias sociaux ou des sites web n'est autorisée qu'avec l'accord préalable des détenteurs des droits. [En savoir plus](#)

### **Terms of use**

The ETH Library is the provider of the digitised journals. It does not own any copyrights to the journals and is not responsible for their content. The rights usually lie with the publishers or the external rights holders. Publishing images in print and online publications, as well as on social media channels or websites, is only permitted with the prior consent of the rights holders. [Find out more](#)

**Download PDF:** 10.08.2025

**ETH-Bibliothek Zürich, E-Periodica, <https://www.e-periodica.ch>**

## Computer-Aided Design of Box Girders Using a Simple Non-Linear Technique

Projet de poutres-caissons par l'emploi d'une simple technique non-linéaire

Entwurf von Kastenträgern mit einem einfachen nicht-linearen Verfahren

### A.R. CUSENS

Head and Prof. of Civil Eng.  
University of Leeds  
Leeds, England



Before going to Leeds in 1979, Tony Cusens was Professor at the University of Dundee for 13 years. His main research field is concrete structures, especially bridges and he is the co-author of two books on bridge deck analysis. He is Vice-chairman of the British Group of IABSE and President of the Concrete Society 1983–84.

### P. LENGYEL

Chief Engineer  
Videoton Fejlesztési Intézet  
Budapest, Hungary



Peter Lengyel, born 1953, is a structural engineer and applied mathematician, who received his degrees at universities in Budapest. He is a candidate of technical sciences in bridge engineering and doctor of numerical analysis. He manages a department of CAD programming and has been involved in FEM research.

## SUMMARY

The paper describes the application of a geometrical, non-linear, finite strip method to the computer-aided design of box girders. It includes two examples of application of the method. A square isotropic plate is analysed, showing excellent correlation with a finite element solution. Then, using this method, the Danube bridge failure of 1969 is re-examined, confirming the mode of failure established by previous authors, but resulting in different numerical values.

## RESUME

Cette étude décrit l'application d'une méthode non-linéaire géométrique de bande finie au projet par ordinateur de poutres-caissons. Elle comprend deux exemples d'application de la méthode. Une plaque carrée isotrope est analysée et montre une corrélation excellente avec une solution par éléments finis. L'analyse de la rupture, en 1969, du pont sur la Danube confirme le mode de rupture établi antérieurement par d'autres auteurs, mais aboutit à des valeurs numériques différentes.

## ZUSAMMENFASSUNG

Diese Arbeit präsentiert die Anwendung einer geometrisch nicht-linearen Methode der finiten Streifen für die rechnerunterstützte Projektierung von Kastenträgern. Sie beinhaltet zwei Anwendungsbeispiele der Methode. Eine Rechteckplatte wird analysiert. Eine vollkommene Korrelation mit der Lösung der Methode der finiten Elemente zeigt sich. Danach wird mit Hilfe dieses Verfahrens der 1969 erfolgte Einsturz der Donaubrücke nochmals analysiert. Die von früheren Autoren angegebenen Bruchursachen werden bestätigt. Es ergeben sich jedoch verschiedene numerische Werte.



## 1. INTRODUCTION

The finite strip method has been applied widely since the early seventies and has been shown to be an efficient tool for the analysis of box girders. The first versions of the method were based on a linear displacement formulation of the finite element procedure using a combination of polynomial and harmonic functions for the solution of simply supported folded plate structures [1]; this was later extended to multi-span structures [6].

The development of a geometrical non-linear finite strip technique has been the subject of research in recent years [3, 4, 8]. However, solutions have been based primarily on special displacement functions and this results in a restricted characterisation of geometrical non-linearity.

The idea of closely following the finite element procedure was put forward by the authors in a previous publication [5]. Since then this technique has been further tested and applied with the development of Fortran programs for different mini- and micro-computers.

This paper is concerned primarily with the presentation of two representative applications of the method. However, a short summary of the technique is given in the Appendix.

The examples in this paper demonstrate the analysis of steel structures with longitudinal stiffeners, simply supported at two opposite ends (Fig. 1). For simple supports, the following conditions are assumed: the vertical displacement ( $w$ ) of the plate is perpendicular to its plane; the transverse rotation ( $\theta$ ) and the transverse displacement ( $u$ ) are zero, while the longitudinal displacement ( $v$ ) is non-zero.

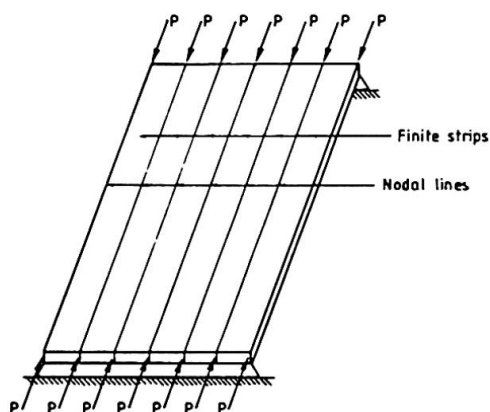


Fig. 1

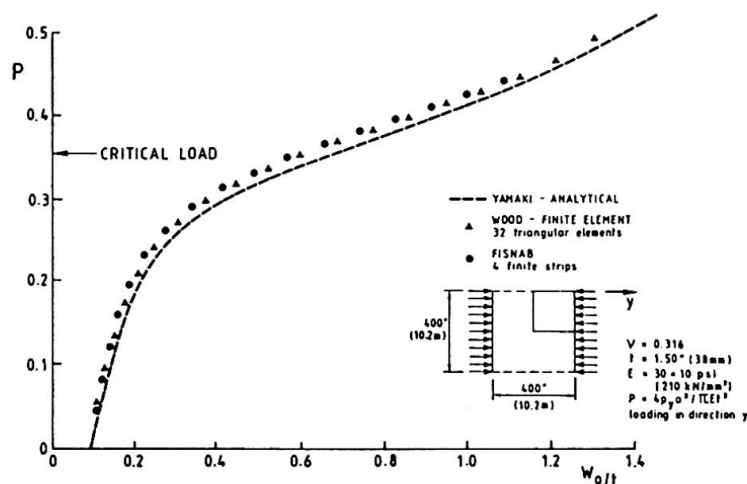


Fig. 2

The aim of the analysis is primarily to investigate the greatest lateral displacement and the corresponding stress distributions of the plate under increasing load in the longitudinal plane.

The examples in this paper were solved by applying only one harmonic; however the effect of more than one harmonic can also be found. In both examples an initial central displacement was assumed by applying a vertical concentrated load  $P_0$  at the mid-point of the plate.

The results were obtained by running the Fortran program FISNAB which has been implemented on Leeds University's PRIME 750 and VIDEOTON's VT 600 computers.

## 2. ANALYSIS OF A SIMPLY SUPPORTED RECTANGULAR PLATE

Figure 2 shows the case of a rectangular plate simply supported at four edges. The support conditions of the horizontally loaded edges have already been described. The unloaded edge conditions were obtained by prescribing the vertical displacement of the plate in these nodal lines as zero, while the other three displacements -  $\theta$ ,  $u$  and  $v$  - were not prescribed.

This is a problem for which several solutions are available in the literature, thus providing useful comparisons. The square plate analysed by Yamaki [12] and Wood [11] is used here. Its dimensions are 400 x 400 in by 1.5 in thick (10 m x 10 m x 38 mm) and the initial central displacement is 0.15 in (3.8 mm). Figure 2 shows the relation between this ratio of the central displacement and plate thickness and the quantity  $P$  characteristic of the compressive loading. This quantity is approximated by Wood [11] and Yamaki [12] as:

$$P = \frac{4p_y a^2}{Et^2}$$

where  $p_y$  is the average compressive stress in direction  $y$ . The dashed line shows the analytical result of Yamaki, triangles denote the result of the finite element analysis of Wood, who investigated one quarter of the plate using 32 triangular elements. The results from the FISNAB program are shown by circles and are based upon the application of four finite strips and one harmonic. Advantage was taken of the symmetrical nature of the problem and one half of the plate only was analysed.

## 3. ANALYSIS OF THE FAILURE OF THE VIENNA DANUBE BRIDGE

3.1 In the evening of 6th November 1969 the Vienna Danube bridge, while under construction, failed at three sections. The bridge had two intermediate supports forming spans of 82, 210 and 120 metres. The structure of the bridge was formed of two torsionally stiff box girders of 7.6 m width and 5.2-7.5 m height, at 15.6 m spacing. The box girders supported a 32 m wide orthotropic plate deck (Fig. 3).

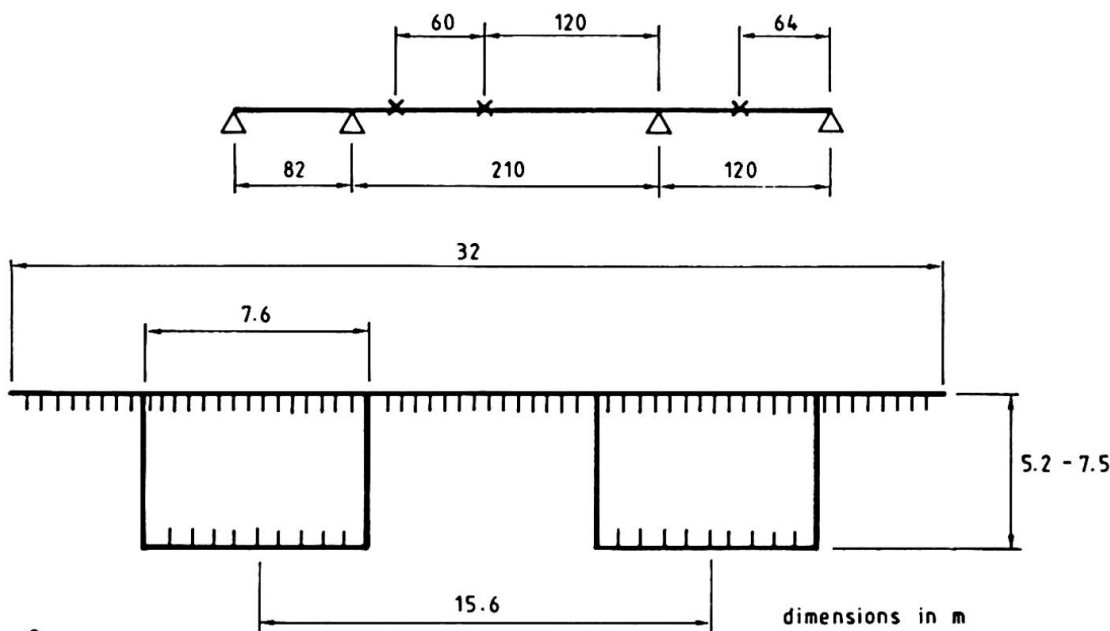


Fig. 3

The collapse of the bridge launched a fierce technical debate especially because the dimensioning and construction were carried out following the current Austrian specifications.



Prof. P. Cicin of Vienna, Prof. K. Sattler of Graz and Prof. P. Roik of Berlin, published different explanations in the journal "Tiefbau" in 1970 [2, 9, 10]. Further research on this problem at the University of Liege was later published by Maquoi and Massonnet [7]. Based primarily on this paper the change of displacement of the lower flange mid-point with increasing longitudinal horizontal loading was analysed together with the stress distribution in the cross-section corresponding to each of the loading values. These results are presented in the following sections.

- 3.2 According to a nearby observatory, the fracture occurred at three cross-sections, at five second intervals, at 8.44 p.m. The middle closing member had been put in at 8 a.m. when the observatory temperature was 4.2°C. The temperature had risen by 2.2°C by 2 p.m., and then decreased by 4.9°C. It is reasonable to assume that at the bridge site a somewhat greater increase of 8-10°C occurred with a later decrease of 12-15°C.

The most important factor in considering the cause of the failure is the greater increase of loading of the bridges compared with the expected load because of:

- a) the significant change of ambient temperature;
- b) the unexpectedly non-uniform distributed dead load.

It is apparent that initially the entire lower flange of the box girder failed and the full collapse of the cross section followed afterwards.

- 3.3 Based on these considerations, Maquoi and Massonnet have analysed the yielding of the lower flange.

The most important aim of the analytical method devised was to take into consideration the essential deviation of the stress distribution from a uniform one in the lower flange. This deviation is caused by three factors:

- a) The shear lag effect, i.e. consideration of the deformations due to the shearing forces;
- b) The curvature of the entire flange, increasing under the compressive forces;
- c) Curvature of the plate between individual longitudinal stiffeners.

The combination of these factors results in the theoretical distribution of the longitudinal stresses of the stiffened plate shown as curve II of Fig. 4. If the effect of c) is omitted, then curve I is obtained, while line A denotes an approximately uniform distribution.

Maquoi and Massonnet took the factors a) and b) into consideration by transforming the lower flange into an orthotropic plate and investigating this with one harmonic according to non-linear analysis. In this way a non-uniform longitudinal stress distribution was obtained. Since this method could not follow exactly the effect c), the authors investigated a segment of plate between two longitudinal stiffeners, which had an initial deformation.

They took into consideration the approximate effect of this curvature by the introduction of an effective plate width. The approximate nature of this investigation was caused by the combination of a final common reducing factor from individual factors from two separate analyses expressed simply as a multiple of the two. Then the work concentrated on the presentation of the two latter multiplying factors. This was done within plate theory by the assumption of the displacement function:

$$w = \cos \frac{x}{a} \cdot \cos \frac{y}{b}$$

Maquoi and Massonnet state in their analysis of the state of collapse that the external, longitudinal stress consisted of:

$$\sigma_{\text{dead load}} = 194 \text{ N/mm}^2 \quad (\text{MPa})$$

$$\sigma_{\text{change in temp.}} = 26 \text{ N/mm}^2$$

forming a total applied stress of:

$$\sigma_{\text{total}} = 220 \text{ N/mm}^2$$

The critical load was:

$$\sigma_{\text{crit}} = 217 \text{ N/mm}^2$$

while the yielding limit was:

$$\sigma_{\text{yield}} = 285 \text{ N/mm}^2$$

As Maquoi and Massonnet obtained:

$$\sigma_1 = 0.811 \quad ; \quad \sigma_2 = 0.848$$

for the two multiplying factors, they derived the value:

$$\sigma_{\text{limit}} = 0.811 \times 0.848 \times 285 = 196 \text{ N/mm}^2$$

i.e., if the stress, assumed to be uniform along the cross-section, reached this value, then at the marginal point of the stress distribution denoted by curve II in Fig. 4, the cross-section yields.

This investigation contains a number of approximations since the simplified analysis is not able to follow exactly the geometrical form of the cross-section.

3.4 Based on the previous analysis it was an interesting task to plot the entire stress distribution of the cross-section as a function of the longitudinal loading using the FISNAB program.

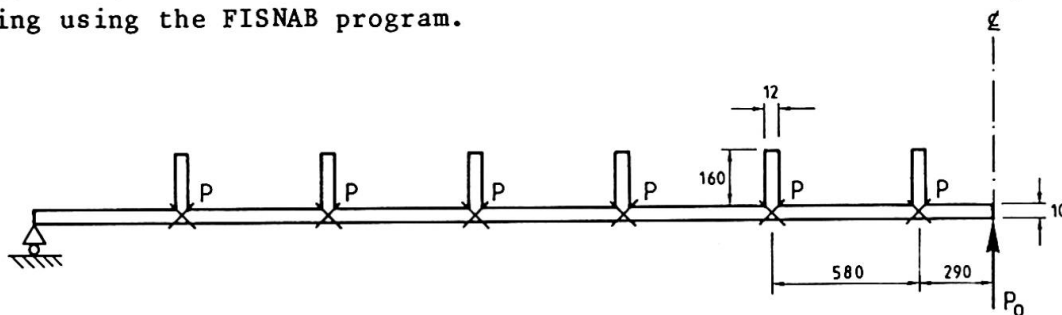


Fig. 5

dimensions in mm

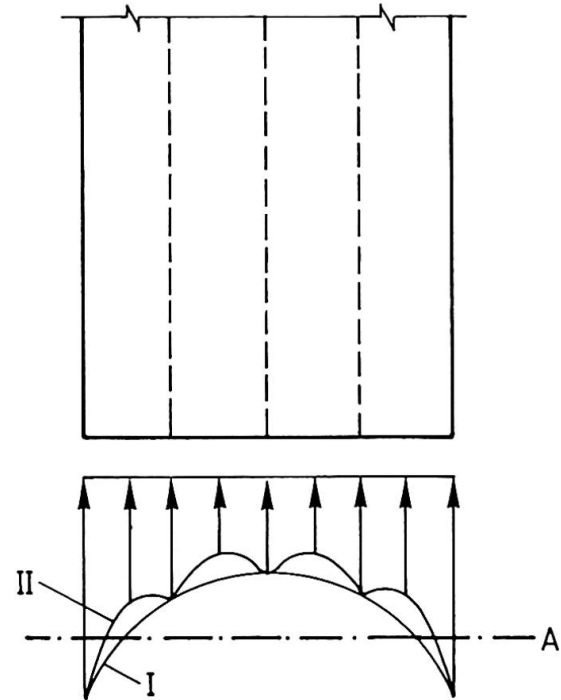


Fig. 4



The lower flange was modelled as shown in Fig. 5 making use of the symmetrical geometry of the section. The two extreme points of the cross-section were assumed to have no vertical displacement because of the supporting effect of the webs. The lower flange was considered to be a part of a box girder segment bounded by two stiff diaphragms, and having no intermediate transverse stiffeners. At the two bounding stiffening diaphragms the flange was assumed to be simply supported. A vertical load applied at the centre point of the plate approximated the initial curvature of the lower flange. The geometrical data of the structure are given in Fig. 5.

By increasing the longitudinal horizontal loading formed by concentrated, longitudinal loads along the nodal lines indicated as denoted in Fig. 5, two graphs have been plotted.

The first, Fig. 6, shows the values of longitudinal stress at the centre of the box girder segment plotted against the applied stress due to the longitudinal loads. The two curves show:

- Maximum stress at the central cross-section of flange;
- Minimum stress in the central cross-section of the flange, i.e., at the central point of the flange.

These values correspond to the maximum values of displacement.

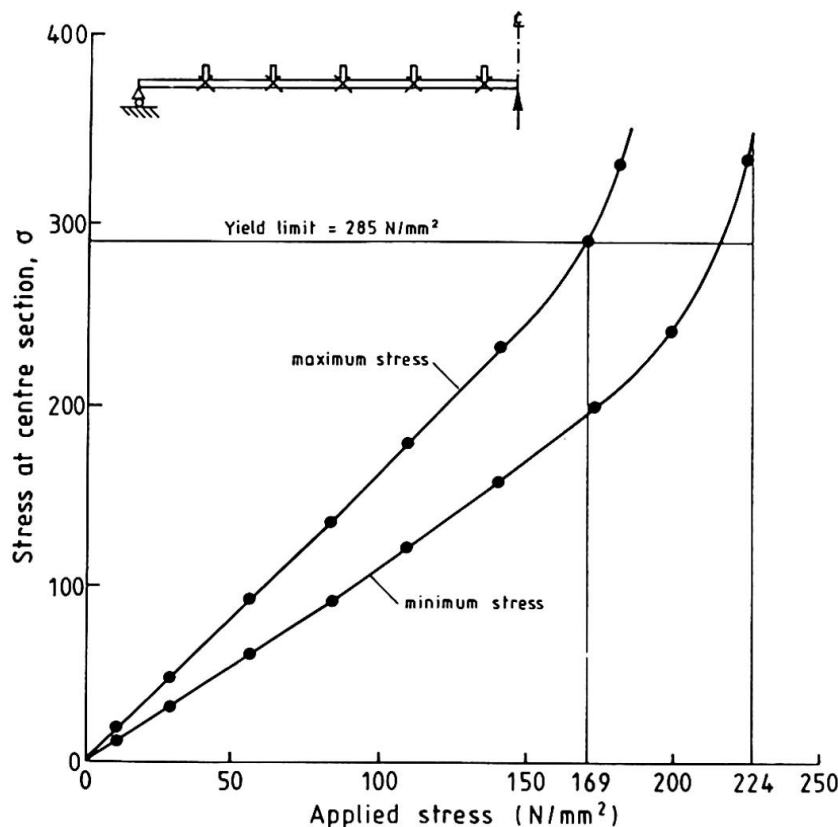


Fig. 6

A horizontal line at the yield value  $285 \text{ N/mm}^2$  is drawn in Fig. 6. The point at which the curve of maximum stress crosses this line is the limiting loading stress corresponding to yielding. This value is  $169 \text{ N/mm}^2$ . The critical load would correspond to a mid-point stress of  $224 \text{ N/mm}^2$ .

Figure 7 shows the distribution of longitudinal stress over the entire cross-section. This figure shows that upon increase of the applied loading



stress, the longitudinal stress increases more rapidly at the line of the cross-section under the webs as compared with the stress increase at the centre line. This means that the curvature of curve I in Fig. 4 is even more pronounced, while the shear lag effect between longitudinal stiffeners (curve II) can also be seen in Fig. 7, particularly at the centre-line.

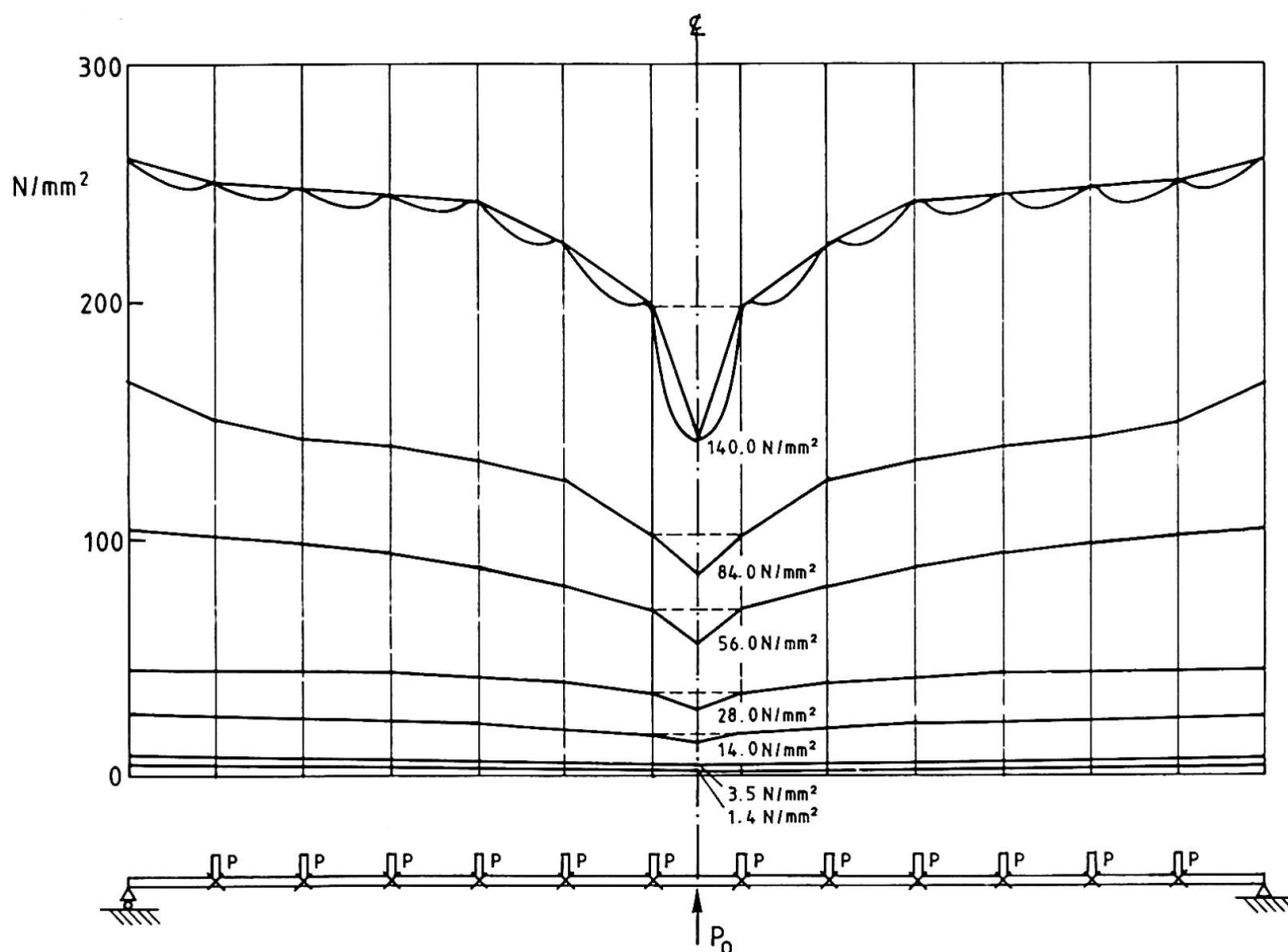


Fig. 7

To summarise, it can be concluded that if the lower flange of the Vienna Danube bridge is analysed by a direct study of the real stress distribution, then:

- the permissible loading stresses given by Sattler [10] are actually  $50 \text{ N/mm}^2$  above the yield limit;
- the limit stress is  $169 \text{ N/mm}^2$ , i.e. smaller than the  $196 \text{ N/mm}^2$  obtained by Maquoi and Massonnet [7];
- the collapse was initiated by yield at the web/flange junction of the lower flange.

#### 4. ACKNOWLEDGEMENT

The development and testing of the method were achieved with the aid of Professor Halász, Head of Department of Steel Structures, Technical University, Budapest. The second example was suggested by Professor Halász in the light of





his own studies of this problem. His help is greatly appreciated.

The facilities of, and permission for publication by, the VIDEOTON Development Institute are gratefully acknowledged.

## 5. REFERENCES

- [1] Y.K. Cheung, Finite Strip Method in Structural Analysis, Pergamon, New York, 1976.
- [2] P. Cicin, Betrachtungen über die Bruchursachen der neuen Wiener Donaubrücke, Tiefbau (665-674), 1970.
- [3] T.R. Graves-Smith and S. Sridharan, A Finite Strip Method for the Post-Locally-Buckled Analysis of Plate Structures, Int. J. Mech. Sci., 20 (833-842), 1978.
- [4] G.J. Hancock, Non-Linear Analysis of Thin Sections in Compression, Research Report R 355, University of Sydney, 1979.
- [5] P. Lengyel and A.R. Cusens, A Finite Strip Method for the Geometrically Non-Linear Analysis of Plate Structures, Int. J. Num. Meths. Engg., Vol. 19 (331-340), 1983.
- [6] Y.C. Loo and A.R. Cusens, The Finite Strip Method in Bridge Engineering, Viewpoint Publications, Cement and Concrete Association, 1978.
- [7] R. Maquoi and Ch. Massonnet, Théorie non-linéaire de la résistance postcritique des grades poutres en caisson raidies. IABSE Publications 31-II, (91-140), 1971.
- [8] R.J. Plank and W.H. Wittrick, Buckling under Combined Loading of Thin, Flat-Walled Structures by a Complex Finite Strip Method, Int. J. Num. Meths. Engg., 8 (323-339), 1974.
- [9] K. Roik, Nochmals: Betrachtungen über die Bruchursachen der neuen Wiener Donaubrücke (1152), 1970.
- [10] K. Sattler, Nochmals: Betrachtungen über die Bruchursachen der neuen Wiener Donaubrücke (948-950), 1970.
- [11] R.D. Wood, The Application of Finite Element Methods to Geometrically Non-Linear Structural Analysis, Ph.D. Thesis, University of Wales, Swansea, 1973.
- [12] N. Yamaki, Postbuckling Behaviour of Rectangular Plates with Small Initial Curvature Loaded in Edge Compression, J. Appl. Mech. (407-414), 1959.

## 6. APPENDIX - THE GEOMETRICAL NON-LINEAR FINITE STRIP METHOD

Consider the finite strip denoted by I having the length of b and the width of a of Fig. A1.

Two nodal lines belong to the strip denoted by i and j. The method assumes four displacement components characterised by the following terms:

$$w(x,y) = \sum_{m=1}^r (\alpha_1 + \alpha_2 x + \alpha_3 x^2 + \alpha_4 x^3) \sin k_m y$$

$$\theta(x,y) = \sum_{m=1}^r (\alpha_2 + 2\alpha_3 + 3\alpha_4 x^2) \sin k_m y$$

$$u(x,y) = \sum_{m=1}^r (\alpha_5 + \alpha_6 x) \sin k_m y$$

$$v(x,y) = \sum_{m=1}^r (\alpha_7 + \alpha_8 x) \cos k_m y$$

where  $k_m = \frac{m\pi}{a}$

The displacement parameters belonging to the strip I form the vector  $\underline{e}^I$ , where:

$$\underline{e}^I = \sum_{m=1}^r \underline{e}_m^I = \sum_{m=1}^r [u_{im}, v_{im}, \theta_{im}, u_{jm}, v_{jm}, w_{jm}, \theta_{jm}]^T$$

These enable us to describe the displacement of nodal lines i and j, utilising the above approximations, by:

$$w_i = \sum_{m=1}^n w_{im} \sin k_m y, \quad w_j = \sum_{m=1}^n w_{jm} \sin k_m y$$

The strain vector of strip I, and harmonic m, contains a linear and non-linear component and takes the form of:

$$\underline{\epsilon}_m^I = \underline{\epsilon}_{om}^I + \underline{\epsilon}_{Nm}^I$$

The corresponding strain-matrix components are:

$$\underline{B}_m^I = \underline{B}_{om}^I + \underline{B}_{Nm}^I$$

where

$$d\underline{\epsilon}_m^I = \underline{B}_m^I d\underline{e}_m^I$$

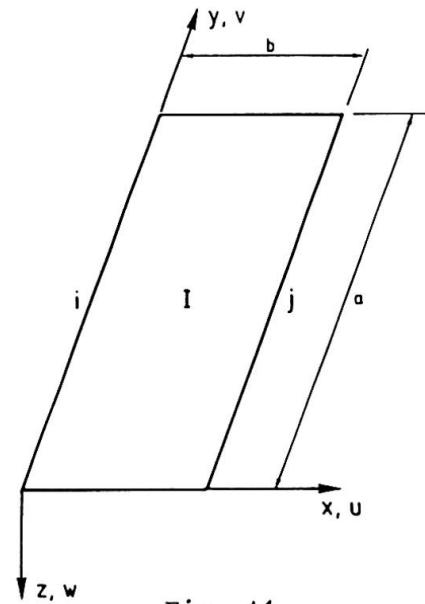


Fig. A1

Following the non-linear finite element solution of [11], the summation of internal and external forces for the total structure and harmonic m results in:



$$\Psi_{-m} = \sum_{I=1}^N \sum_{n=1}^r \int_0^a \int_0^b (B_n^I)^T \underline{\sigma}_{-m}^I dx dy - \sum_{I=1}^N \underline{r}_{-m}^I = 0$$

Here the vector  $\underline{\sigma}_{-m}^I$  contains the stress components, the vector  $\underline{r}_{-m}^I$ , the loading components for harmonic  $m$  and strip  $I$ .

Making use of the connection of:

$$\underline{\sigma}_{-m}^I = \underline{D}^I \underline{B}_m^I \underline{e}_{-m}^I$$

where  $\underline{D}^I$  denotes the elasticity matrix,  $\underline{B}_m^I$ , the strain matrix for non-differential quantities, the following expression is obtained:

$$\Psi_{-m} = \sum_{I=1}^N \sum_{n=1}^r \int_0^a \int_0^b (B_n^I)^T \underline{D}^I \underline{B}_m^I \underline{e}_{-m}^I dx dy - \sum_{I=1}^N \underline{r}_{-m}^I$$

where again:

$$\underline{B}_m^I = \underline{B}_{om}^I + \underline{B}_{Nm}^I (\underline{e}_1^I, \underline{e}_2^I, \dots, \underline{e}_r^I)$$

The state of equilibrium of the analysed structure is characterised by the vector series of displacement amplitudes,  $\underline{e}_1, \underline{e}_2, \dots, \underline{e}_r$  for the whole structure resulting in a zero vector for:

$$\underline{\Psi} = \sum_{m=1}^r \underline{\Psi}_{-m}$$

The Newton-Raphson method is applied, represented here by:

$$\frac{d\Psi}{d\underline{e}_{-m}^I} = \underline{K}_{Tm}^I$$

where:

$$\underline{K}_{Tm}^I = \underline{K}_{om}^I + \underline{K}_{Nm}^I + \underline{K}_{\sigma m}^I$$

and

$$\underline{K}_{om}^I + \underline{K}_{Nm}^I = \sum_{n=1}^r \int_0^a \int_0^b (B_n^I)^T \underline{D}^I \underline{B}_m^I dx dy$$

with

$$\underline{K}_{\sigma m}^I = \sum_{n=1}^r \int_0^a \int_0^b d(B_{Nm}^I [\underline{e}_1^I, \underline{e}_2^I, \dots, \underline{e}_r^I])^T \underline{\sigma}_{-m}^I dx dy$$

and

$$\underline{K}_{\sigma m}^I = \underline{K}_{\sigma m}^I \cdot d\underline{e}_{-m}^I$$

The last equations define an iterative solution for the determination of vectors  $\underline{e}_m$  ( $m = 1, 2, \dots, r, I = 1, 2, \dots, N$ ) resulting in equilibrium based on a non-linear relationship between strains and displacements.